Table 2. Upregulated Genes in ALS Motor Neurons (Top 30)

GeneBank No.	Gene Name	Fold Change (ALS/control)
NM_003419	Zinc finger protein 10 (KOX 1)	8.86
U91618	Neurotensin/neuromedin N precursor	8.33*
NM_004651	Ubiquitin-specific protease 11	8.13
D86984	KIAA0231	7.31*
A26792	Ciliary neuronotrophic factor (CNTF)	6.76
M77830	Desmoplakin I & II (DSP; DPI & DPII)	6.10
NM_005622	SA (rat hypertension-associated) homolog	5.47
NM_004733	Acetyl-coenzyme A transporter	5.33
NM_000021	Presenilin 1 (Alzheimer disease 3)	4.96
K03020	Phenylalanine-4-hydroxylase (PAH)	4.95*
AF016268	Death receptor 5 (DR5); cytotoxic TRAIL receptor, TNFR10b	4.91*
M74091	G1/S-specific cyclin C (CCNC)	4.82*
NM_000275	Oculocutaneous albinism II	4.78
AF000936	SH3-binding protein 2	4.73*
NM_000384	Apolipoprotein B	4.70
M63099	Interleukin-1 receptor antagonist	4.66*
M57730	Ephrin-A1	4.57*
L19067	NF-κ B transcription factor p65 subunit	4.52*
U66838	Cyclin A1 (CCNA1)	4.51*
NM_005021	Ectonucleotide pyrophosphatase/phosphodiesterase 3	4.48
NM_001550	Interferon-related developmental regulator 1	4.45
L25851	Integrin alpha E precursor (ITGAE)	4.43*
X16416	C-abl1 protooncogene	4.41
U08015	Transcription factor NF-ATc	4.40*
U44378	Mothers against dpp homolog 4 (SMAD4)	4.35*
NM_005067	Seven in absentia (Drosophila) homolog 2	4.22
J04536	Leukosialin precursor; sialophorin	4.19*
X06745	DNA polymerase alpha catalytic subunit	4.15*
U09564	Serine kinase	4.09*
U37139	β 3-endonexin	4.06*

Gene expression levels are expressed as means of fold-change, which is calculated by dividing the signals of each ALS sample by those of control samples, in the 5 or 10 (denoted by asterisk) patients with ALS.
ALS = amyotrophic lateral sclerosis.

metabolism, and cytoskeletal architecture were downregulated. The functional categories of secreted and extracellular communication proteins and cell cycle regulators were characteristically upregulated. A complete list of the differentially expressed genes is available online at http://www.med.nagoya-u.ac.jp/neurology/index.html.

Differential Gene Expression Profiles between Spinal Motor Neurons and Ventral Horn Homogenates of Amyotrophic Lateral Sclerosis

To compare the expression profile of motor neurons with that of spinal ventral horn homogenates, we performed cluster analyses. Because the patterns of gene expression from microarray analysis are impossible to discern by eye, data analysis software (Acuity 3.0 software; Axon Instruments) was used based on the dimensionality of the data: hierarchical clustering for high dimensional gene space and principal component analysis and SOM for low one. Hierarchical clustering clearly discriminated the expression profile of isolated motor neurons from that of ventral horn homogenates, showing two grouped branches of the dendrogram with a correlation coefficient of 0.446 (Fig 2A). Moreover, a principal component analysis confirmed the distinction of gene expression profiles between spinal motor neurons and ventral horns (see Fig 2B). The gene expression profile of motor neurons was clustered into a single cluster by the two clustering algorithms, which was well separated from that of spinal ventral horn gray matter, suggesting a relatively uniform degenerating process in spinal motor neurons in ALS.

Motor Neuron–Specific Gene Expression Profiles Identified by the Self-Organizing Map Analysis

To further analyze the expression pattern specific to spinal motor neurons, a SOM was produced as a nonhierarchical clustering.[24,25] The examined genes were subdivided into 25 clustered categories, and the selected genes are shown in a certain group of the SOM (see Fig 2C, Table 6). The genes contained in the clusters reflect the expression pattern in spinal motor neurons as well as that in spinal ventral horns, and these selected genes are somehow different from those in Tables 2 to 5 because of the different bases of classification. Clustering of the SOM showed motor neu-

Table 3. Downregulated Genes in ALS Motor Neurons (Bottom 30)

GeneBank No.	Gene Name	Fold Change (ALS/control)
NM_004378	Cellular retinoic acid–binding protein 1 (CRABP1)	0.12
NM_004430	Early growth response 3 (EGR3)	0.14
NM_005558	Ladinin 1	0.15
NM_003603	Arg/Abl-interacting protein ArgBP2	0.15
NM_000117	Emerin (Emery-Dreifuss muscular dystrophy)	0.15
NM_004357	CD151 antigen	0.15
X06820	Ras homolog gene family member B (RHOB)	0.15*
NM_003834	Regulator of G-protein signalling 11	0.16
NM_002960	S100 calcium-binding protein A3	0.16
NM_006289	Talin	0.16
NM_000964	Retinoic acid receptor, α	0.17
NM_002391	Midkine	0.17
M96944	Paired box protein PAX-5	0.17*
M74178	Hepatocyte growth factor–like protein	0.17*
NM_003822	Nuclear receptor subfamily 5, group A, member 2	0.17
NM_001188	BCL2-antagonist/killer 1; Bak	0.18
NM_000733	CD3E antigen, epsilon polypeptide (TiT3 complex)	0.18
NM_000408	Glycerol-3-phosphate dehydrogenase 2 (mitochondrial)	0.18
NM_000156	Guanidinoacetate *N*-methyltransferase	0.18*
M11886	Major histocompatibility complex, class I, C	0.18*
NM_003865	Homeo box (expressed in ES cells) 1	0.18
M36340	ADP-ribosylation factor 1 (ARF1)	0.18*
NM_001725	Bactericidal/permeability-increasing protein	0.18
NM_005334	Host cell factor C1 (VP16-accessory protein)	0.19
NM_004192	Acetylserotonin *O*-methyltransferase–like	0.19
NM_002684	Postmeiotic segregation increased 2–like 11	0.19
M11233	cathepsin D precursor (CTSD)	0.19*
NM_002313	Actin binding LIM protein 1	0.19
NM_002196	Insulinoma-associated 1	0.19
NM_002277	Keratin, hair, acidic, 1	0.19

Gene expression levels are expressed as means of fold-change, which is calculated by dividing the signals of each ALS sample by those of control samples, in the 5 or 10 (denoted by asterisk) patients with ALS.
ALS = amyotrophic lateral sclerosis.

ron–specific upregulated and downregulated gene expression commonly observed in five patients.

Clusters 1 (SOM1) and 6 (SOM6) contains 110 and 169 genes, respectively, that generally are downregulated in spinal motor neurons in all five cases examined, and those are known to be involved in the functional category of cell surface antigens and cell receptors, transcription, and cytoskeleton, whereas clusters 24 (SOM24) and 25 (SOM25) have 191 and 93 genes, respectively, that are predominantly upregulated in spinal motor neurons in all cases and belong to the functional category of cell signaling with extracellular communication, and cell death–associated proteins. The pattern of subcellular localization of their gene products also confirms the characteristics of the functional categories of upregulated and downregulated genes, that is, that plasma membrane and cytoskeletal proteins are more downregulated, and extracellular secreted proteins are more upregulated, in ALS motor neurons. All the genes listed in Table 3 are included in SOM1 and SOM6, whereas SOM24 and SOM25 do not contain all of the genes listed in Table 2. The former group of genes, with downregulation in motor neurons, included BCL2-antagonist/killer 1 (Bak) and TrkC receptor. Regarding genes related to transcription, early growth response 3 (EGR3), cellular retinoic acid–binding protein 1 (CRABP1), retinoic acid receptors, and Musashi 1 were included in SOM1 and SOM6 as downregulated genes. The expression of dynactin and microtubule-associated proteins (MAPs), which belong to the functional category of cytoskeleton and axonal transport, was downregulated in ALS motor neurons. On the other hand, KIAA0231 and acetyl-coenzyme A transporter were classified into the upregulated genes in motor neurons of ALS. Regarding genes related to cell death, the expression of cyclins A1 and C, death receptor 5 (DR5), and interleukin-1 receptor antagonist was upregulated together with that of NF-κB, tumor necrosis factor (TNF) receptor–associated factor 6 (TRAF6), and caspase-1, -3, and -9 in SOM24 and SOM25. For genes in the category of trophic factor cell signaling with extracellular communication, CNTF, HGF, and glial cell line–derived neurotrophic factor (GDNF) were upregulated in ALS motor neurons, whereas midkine was downregulated. The expression of vascular endothelial growth factor as

Table 4. Upregulated Genes in Spinal Ventral Horns of ALS (Top 30)

GeneBank	Gene Name	Fold Change (ALS/control)
NM_000508	Fibrinogen, A α polypeptide	8.23
D86984	KIAA0231	6.09
NM_001801	Cysteine dioxygenase, type I	5.81
X02544	α-1-Acid glycoprotein 1 precursor	5.59
NM_001973	ELK4, ETS-domain protein (SRF accessory protein 1)	5.12
NM_000021	Presenilin 1 (Alzheimer disease 3)	5.00
NM_002097	General transcription factor IIIA	4.96
U08015	Transcription factor NF-ATc	4.96
M57730	Ephrin-A1	4.88
U91618	Neurotensin/neuromedin N precursor	4.79
AF000936	SH3-binding protein 2	4.50
NM_002949	Mitochondrial ribosomal protein L12	4.11
NM_002386	Melanocortin 1 receptor	4.03
NM_001991	Enhancer of zeste (Drosophila) homolog 1	3.93
NM_000947	Primase, polypeptide 2A (58kDa)	3.92
NM_000239	Lysozyme (renal amyloidosis)	3.88
NM_001550	Interferon-related developmental regulator 1	3.67
NM_004602	Staufen (Drosophila, RNA-binding protein)	3.66
NM_000063	Complement component 2	3.58
NM_004651	Ubiquitin-specific protease 11	3.54
NM_000397	Cytochrome b-245, β polypeptide	3.51
NM_002056	Glutamine-fructose-6-phosphate transaminase 1	3.41
L25851	Integrin α E precursor (ITGAE)	3.36
NM_004616	Transmembrane 4 superfamily member 3	3.21
NM_003720	Down syndrome critical region gene 2	3.18
J04536	leukosialin precursor; sialophorin	3.15
X06745	DNA polymerase alpha catalytic subunit	3.15
K03020	Phenylalanine-4-hydroxylase (PAH)	3.14
NM_001329	C-terminal binding protein 2	3.14
NM_000276	Oculocerebrorenal syndrome of Lowe	3.13

Gene expression levels are expressed as means of fold-change, which is calculated by dividing the signals of each ALS sample by those of control samples, in the five patients with ALS.
ALS = amyotrophic lateral sclerosis.

well as NT-3 was unchanged. Furthermore, the genes whose expression was altered significantly in spinal ventral horn homogenates as shown in Tables 4 and 5 showed similar alterations to some extent in the remaining motor neurons. However, the upregulated genes, such as integrin αE and sialophorin for cell adhesion, which were demonstrated to be spinal ventral horn–derived (see Table 4) as well as spinal motor neuron–derived (Table 2) genes, were not sorted out into SOM24 and SOM25, indicating that their upregulation occurred predominantly in glial cells.

Data Confirmation with Quantitative Real-Time Reverse Transcription Polymerase Chain Reaction, In Situ Hybridization, and Immunohistochemistry

To assure the validity of the gene expression levels detected by microarray analysis, we performed quantitative real-time RT-PCR analysis on some genes of interest using a TaqMan PCR system. Because LCM-isolated motor neurons did not contain enough RNA to perform real-time RT-PCR analysis, only selected genes were assessed in motor neurons, and for other genes the spinal ventral horn homogenates were used as the template for quantitative RT-PCR. When the extent of increase or decrease of gene expression levels was expressed as the ratio of the genes of interest to GAPDH, acetyl-CoA transporter and KIAA0231 were significantly increased 3.1-fold ($p < 0.001$) and 3.3-fold ($p < 0.01$) in spinal motor neurons of ALS, respectively (Fig 3). EGR3 expression decreased to 0.27-fold ($p < 0.01$) in ALS motor neurons. These mRNA alterations were also detected at comparable levels when using spinal ventral horn homogenates of ALS (acetyl-CoA transporter, 1.8-fold increase [$p < 0.005$]; KIAA0231, 2.3-fold increase [$p < 0.05$]; and EGR3, 0.41-fold decrease [$p < 0.01$]). In addition, the gene expression of Bak and TrkC was downregulated 0.53-fold ($p < 0.01$) and 0.40-fold ($p < 0.05$) in ALS, respectively. Moreover, increases of ephrin A1 and cyclin C expression were observed to the extents of 2.5-fold ($p < 0.05$) and 4.9-fold ($p < 0.01$), whereas dynactin 1 mRNA was downregulated 0.44-fold ($p < 0.01$), and CRABP1 mRNA was also downregulated to 0.59-fold ($p < 0.01$) in ALS.

To further verify the localization and extent of expression of genes of interest, we performed in situ hy-

Table 5. Downregulated Genes in Spinal Ventral Horns of ALS (Bottom 30)

GeneBank	Gene Name	Fold Change (ALS/control)
NM_000843	Glutamate receptor, metabotropic 6	0.22
NM_000730	cholecystokinin A receptor	0.24
NM_003134	Signal recognition particle 14kDa	0.26
NM_003163	Syntaxin 1B	0.27
NM_006476	ATP synthase, H+ transporting, mitochondrial F1F0, subunit g	0.27
NM_001610	Acid phosphatase 2, lysosomal	0.28
NM_003108	SRY (sex determining region Y)-box 11	0.29
NM_001446	Fatty acid binding protein 7, brain	0.30
NM_004583	RAB5C, member RAS oncogene family	0.31
NM_001125	ADP-ribosylarginine hydrolase	0.31
NM_003320	Tubby (mouse) homolog	0.31
NM_001731	B-cell translocation gene 1, antiproliferative	0.31
NM_000999	Ribosomal protein L38	0.32
NM_004128	General transcription factor IIF, polypeptide 2 (30kDa subunit)	0.32
NM_001765	CD1C antigen, c polypeptide	0.32
NM_004430	Early growth response 3 (EGR3)	0.33
K00558	Tubulin, α, ubiquitous	0.33
NM_006732	FBJ murine osteosarcoma viral oncogene homolog B	0.33
NM_002040	GA-binding protein transcription factor, α subunit (60kDa)	0.34
NM_006161	Neurogenin 1	0.35
NM_002684	Postmeiotic segregation increased 2–like 11	0.35
NM_000801	FK506-binding protein 1A (12kDa)	0.35
NM_001051	Somatostatin receptor 3	0.35
NM_005017	Phosphate cytidylyltransferase 1, choline, alpha isoform	0.36
NM_004927	Chromosome 11 open reading frame 4	0.36
NM_000046	Arylsulfatase B	0.37
NM_004378	Cellular retinoic acid–binding protein 1 (CRABP1)	0.37
NM_001998	Fibulin 2	0.38
NM_001839	Calponin 3, acidic	0.38
NM_001183	ATPase, H+ transporting, lysosomal, subunit 1	0.39

Gene expression levels are expressed as means of fold-change, which is calculated by dividing the signals of each ALS sample by those of control samples, in the five patients with ALS.
ALS = amyotrophic lateral sclerosis.

bridization on selected genes. The mRNAs for acetyl-CoA transporter, KIAA0231, and EGR3 were localized in the remaining motor neurons (Fig 4). Spinal motor neurons overexpressed acetyl-CoA transporter and KIAA0231 in ALS, whereas EGR3 was underexpressed. Moreover, TrkC, CRABP1, Bak, and dynactin 1 gene expression was found in motor neurons, and those signals were reduced in ALS. DR5 signals were increased in motor neurons in ALS. Cyclin C signals with punctate immunoreactivity were increased in the cytoplasm as well as in nuclei in ALS motor neurons. The nuclear staining of motor neurons for cyclin C was more prominent in ALS compared with controls.

Discussion

Although reports about differential gene expression using the postmortem spinal cords, including those of patients with ALS, have been published,[26,27] the precise gene expression profiles of the degenerating motor neurons themselves have remained to be elucidated. Laser-captured dissection of motor neurons and subsequent microarray analysis are the most appropriate approaches to understanding the motor neuron–specific gene expression profile related to the motor neuron degeneration process in sporadic ALS, because these approaches eliminate bias of motor neuron loss, reactive astroglial proliferation, and other cellular reactions. Indeed, serine kinase has been reported to be underexpressed in ALS spinal cord gray matter,[27] but this study showed it was overexpressed in isolated motor neurons, suggesting that the reported underexpression in whole gray matter was influenced by the decreased motor neuron population. In contrast, cathepsin D expression was downregulated in the ALS motor neurons in this study, whereas it was increased in spinal cord gray matter in a previous report,[27] indicating its upregulation in glial cells. In addition, clustering analyses showed that the gene expression profile in the spinal motor neurons was substantially different from that in the whole homogenates of spinal ventral horn gray matter.

The overall microarray analysis using spinal ventral horn homogenates showed gene expression changes in less than 1% of genes examined with more genes showing increased than decreased expression. On the other hand, the motor neuron–specific microarray analysis

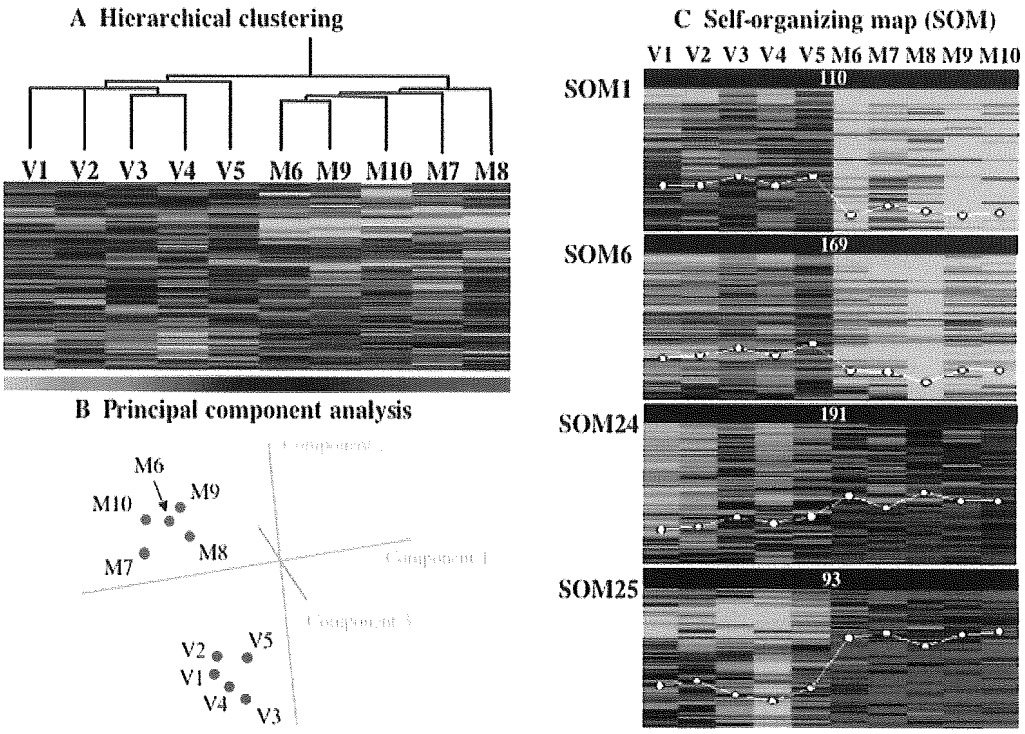

Fig 2. Clustering of gene expression in spinal motor neurons and spinal ventral horns. (A) Hierarchical clustering of gene expression in spinal motor neurons and ventral horns. The dendrogram was produced by hierarchical clustering of relative expression levels of 4,845 genes (rows) in five spinal homogenate and five motor neuron samples (columns) in making a total of 48,450 data points. Visual representation is shown with green representing downregulated (<0.44), black representing intermediate, and red representing upregulated (>2.28). The hierarchical clustering successfully detects two large clusters of amyotrophic lateral sclerosis (ALS), discriminating between spinal homogenates of ventral horns (samples V1 [ALS1], V2 [ALS10], V3 [ALS3], V4 [ALS14], and V5 [ALS13]) and motor neurons (samples M6 [ALS1], M7 [ALS10], M8 [ALS14], M9 [ALS11], and M10 [ALS7]), with a correlation coefficient of 0.446 at the branching point. (B) Principal component analysis of spinal motor neurons and ventral horns. Principal component analysis by six components for the 4,845 genes shows two main clusters consisting of spinal motor neurons (M6–10) and homogenates (V1–5). The number of patients corresponds to those in the dendrogram. (C) Self-organizing map (SOM) analysis of spinal motor neurons and ventral horns. The 4,845 genes are grouped into 25 clusters, the optimal size of which is calculated from gap statistics analysis. In SOM1 and SOM6, most genes are downregulated and in SOM24 and SOM25 the majority of genes are upregulated commonly in isolated motor neurons of five cases (M6–10). The numbers of genes are given at the top, and selected genes are listed for clusters 1, 6, 24, and 25 in Table 6.

showed that the proportion of significantly downregulated genes was 3% of the examined genes, whereas that of upregulated genes was one third of the downregulated genes. Moreover, the genes found to be downregulated specifically in motor neurons were not found to be downregulated in ventral horns, except for three genes with high expression levels. These results strongly support the notion that microarray analysis of laser-captured isolated spinal motor neurons has an advantage especially for the detection of motor neuron–specific downregulated transcripts.

In the differentially expressed genes, cell death–associated genes and genes related to cell signaling were characteristically upregulated in ALS motor neurons, whereas the genes categorized into cytoskeleton and transcription were downregulated. In the prominently altered genes of interest related to the cell death pathway, acetyl-coenzyme A transporter, which has been cloned and shown to encode a protein with multitransmembranous spanning domains,[28] was overexpressed in ALS motor neurons. Acetyl-CoA transporter functions as a cofactor for acetylation of gangliosides as well as vesicular transport of acetylcholine, which is synthesized from acetyl-CoA and choline. Acetylation has been documented to suppress proapoptotic activity of GD3 ganglioside, which increased in ALS neural tissues, as previously shown.[29,30] These results suggest that enhanced expression of acetyl-CoA transporter may be related to the antiapoptotic mechanism for cholinergic motor neuron degeneration in ALS.

Table 6. Selected Genes Characterized by SOM (select each 15)

GeneBank	Gene Name	Fold Change (ALS/control)
SOM1/6: genes downregulated in ALS motor neurons		
NM_002695	Polymerase (RNA) II (DNA directed) polypeptide E (25kD)	0.20
M24857	Retinoic acid receptor gamma 1 (RAR-γ 1)	0.20
NM_002375	Microtubule-associated protein 4	0.20
NM_001651	Aquaporin 5	0.21
NM_003178	Synapsin II	0.22
NM_004624	Vasoactive intestinal peptide receptor 1	0.23
NM_001740	Calbindin 2, (29kD, calretinin)	0.24
M73812	G1/S-specific cyclin E (CCNE)	0.25
NM_003206	Transcription factor 21	0.25
NM_004082	Dynactin 1 (p150)	0.30
U05012	TRK-C; NT-3 growth factor receptor precursor	0.31
NM_003632	Contactin associated protein 1	0.32
NM_005910	Microtubule-associated protein tau	0.49
NM_002373	Microtubule-associated protein 1A	0.51
NM_002442	Musashi (Drosophila) homolog 1	0.52
SOM24/25: genes upregulated in ALS motor neurons		
M60718	Hepatocyte growth factor (HGF)	3.42
L20814	Glutamate receptor subunit 2 (GLUR-2)	3.34
K02268	β-neoendorphin-dynorphin precursor	3.13
L19063	Glial cell line–derived neurotropic factor (GDNF)	3.08
NM_005543	Insulin-like 3	2.79
J04088	DNA topoisomerase II alpha (TOP2A)	2.58
M22489	Bone morphogenetic protein 2A (BMP2A)	2.57
U51004	Hint protein; protein kinase C inhibitor	2.26
M87507	Caspase 1, interleukin-1 β convertase precursor	2.21
NM_006196	Poly(rC)-binding protein 1	2.16
L29511	Growth factor receptor–bound protein 2	2.04
U78798	TRAF6	1.98
NM_001229	Caspase 9, apoptosis-related cysteine protease	1.89
U84388	Caspase and rip adaptor with death domain (CRADD)	1.83
U13737	Caspase-3	1.77

Gene expression levels are expressed as means of fold-change, which is calculated by dividing the signals of each ALS sample by those of control samples, in the five patients with ALS. Genes listed in Tables 2 and 3 are excluded.
SOM = self-organizing map.

KIAA0231 was one of the mostly overexpressed genes in ALS motor neurons, but the function of this gene product is not known.

In the greatly downregulated genes of interest related to transcription, EGR3, whose expression was remarkably reduced in motor neurons of ALS, is a zinc-finger immediate-early transcription factor that is important for neurotrophin-3 (NT-3) regulation. It is known that EGR3 knockout mice develop gait ataxia, scoliosis, resting tremors, and ptosis due to the degeneration of muscle spindles, through disruption of NT-3 regulation.[31] In ALS motor neurons, TrkC receptor for NT-3 was underexpressed, whereas NT-3 expression was not changed. The finding about TrkC-null mutant and NT-3–null mutant mice show that NT-3-TrkC signaling is required to maintain Ia afferent central synapses of DRG neurons.[32] The marked downregulation of EGR3 in spinal motor neurons may disrupt sensory-motor connections by decreasing NT-3-TrkC signaling, resulting in motor neuron degeneration.

For neurotrophic support for ALS motor neurons, this study showed the overexpression of CNTF, GDNF, and HGF involved in the functional category of cell signaling, suggesting that these neurotrophic factors would be secondarily and compensatorily upregulated after motor neuron degeneration. Indeed, GDNF expression has been reported to increase in the spinal cords and decrease in the muscles of sporadic ALS patients.[33] In contrast with these neurotrophic factors, midkine was one of the significantly downregulated neurotrophic factors. Because midkine plays important roles in promotion of neuronal survival as well as modulation of neuromuscular junctions,[34] its underexpression may be related to motor neuron degeneration. In addition, the gene expression of vascular endothelial growth factor, which has been identified as a critical factor for motor neuron degeneration,[35–37] did not change significantly in gene expression in this study. SOD1 gene expression was not altered in spinal motor neurons and ventral horns. Moreover, the gene expres-

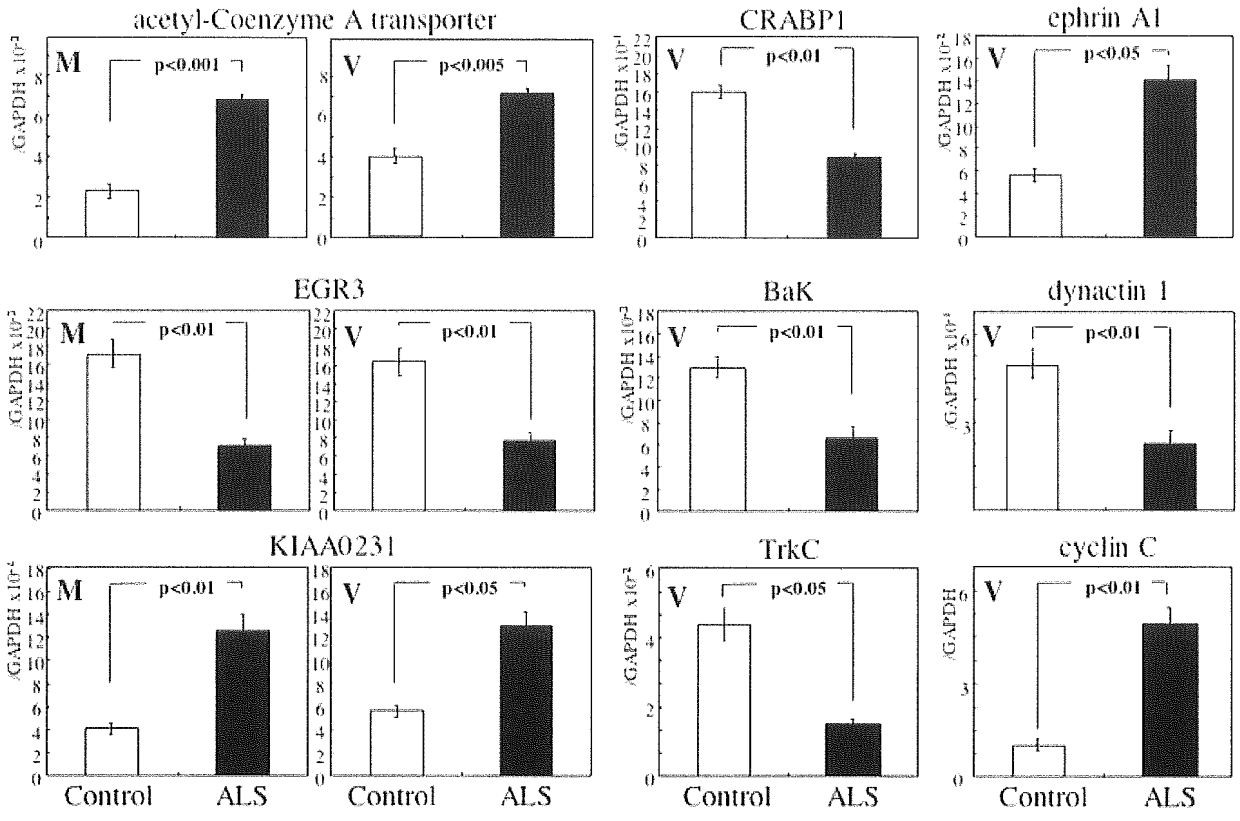

Fig 3. Quantitative real-time reverse transcription polymerase chain reaction verification of the selected genes. Expression levels of acetyl-coenzyme A transporter, EGR3, KIAA0231, CRABP1, Bak, TrkC, ephrin A1, cyclin C, dynactin 1, and GAPDH were measured using spinal motor neurons (M) and ventral horns (V), and those of the target genes were normalized against the GAPDH level. The relative expression levels are expressed as mean ± standard error for 13 amyotrophic lateral sclerosis (ALS) cases and 11 controls. Gene names (Genebank accession number), primers and probe sequences (forward primer, reverse primer, and TaqMan probe; 5' to 3' sequence) were as follows: [acetyl-CoA transporter: D88152] (GGGTTACTTTTTGGGCAATG, AACGATTCCTCTGGGTTGAG, FAM-TTGGCCCTTGAATCTGCCGA-TAMRA); [Bak: NM_001188] (CTGGAAGATCAGCACCCTAAG, CCCCTCTCCTAGTAGGTCCTG, FAM-TGCTCCCATTCCTCCCTCCG-TAMRA); [CRABP1: NM_004378] (TGCAGGAGTTTAGCCACTTG, CTCACGGGTCCAGTAGGTTT, FAM- TGAGAACAAGATCCACTGCACCCA-TAMRA); [cyclin C: M74091] (TGAGCAGTGGAAGAATTTCG, ACCCTGCTCTCCTTCACTGT, FAM- TGCCAAAACCAAAACCACCTCCA-TAMRA); [dynactin 1: NM_004082] (ATGTGAATCGGGAACTGACA, GGGCCTTAGTCTCAGCAAAC, FAM- TGGAGAGGCAACAGCAGCCAC-TAMRA); [EGR3: NM_004430] (CTTCCCCATGATTCCTGACT, TTGAATGCCTTGATGGTCTC, FAM-TTCCAGGGCATGGACCCCAT-TAMRA); [ephrin A1: M57730] (GGCAAGGAGTTCAAAGAAGG, TCACCTTCAACCTCAAGCAG, FAM- CCATCCACCAGCATGAAGACCG-TAMRA); [GAPDH: NM_002046] (TCAAGAAGGTGGTGAAGCAG, GGTGTCGCTGTTGAAGTCAG, FAM-CCTCAAGGGCATCCTGGGCT-TAMRA); [KIAA0231: D86984] (CAACGGTCTTCCAGACAATG, GAGGTTGACCAGCTGTGAGA, FAM-TCCCAGAGGTGAAGCTGCCCTCTAMRA); and [TrkC: U05012] (TGAGAACCCCCAGTACTTCC, TCAGCACGATGTCTCTCCTC, FAM-CTGCCACAAGCCGGACACGT-TAMRA).

sion level of GluR2 was upregulated, as shown by its classification in SOM25, but the expression of its editing enzyme (adenosine deaminase, RNA-specific, 2; ADAR2) was not altered in this study, although the editing efficiency of GluR2 mRNA has been demonstrated to be low in spinal motor neurons of ALS.[38]

Genes subject to transcriptional regulation constitute a crucial part of the whole human genome as demonstrated by human genome projects.[39] In addition to the gene expression of EGR3, the gene expression of retinoic acid receptor α and γ together with cellular retinoic acid–binding protein 1 (CRABP1), and Musashi 1, all of which are known to be inducers of neuronal differentiation,[40,41] was downregulated in spinal motor neurons of ALS. The dysregulation of retinoid receptor and retinol binding protein has been reported in the postmortem spinal cords of ALS and SOD1 mutant mice.[17,26] These interesting results imply the potential involvement of the differentiation signals in maintaining motor neuron integrity, which

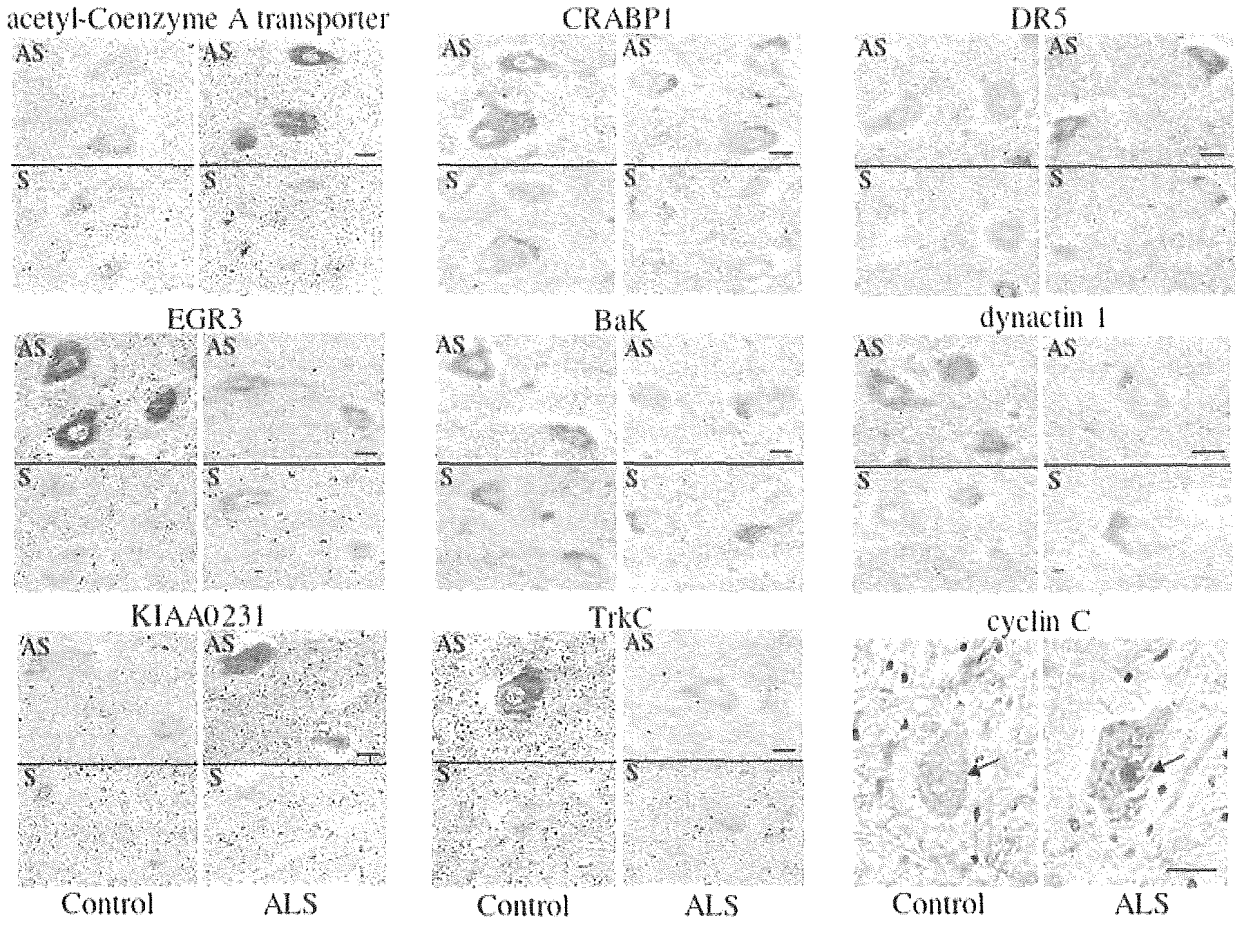

Fig 4. In situ hybridization and immunohistochemistry of the selected genes. Representative in situ hybridization is shown for acetyl-COENZYMEA transporter, EGR3, KIAA0231, CRABP1, Bak, TrkC, DR5, and dynactin 1. The antisense probe (AS) detects positive signals for the expression of each gene in spinal motor neurons for ALS and/or controls, but the sense probe (S) does not. Lipofuscin granules are seen as yellowish granules. Immunohistochemistry was preformed for cyclin C, and nuclear staining was prominent in ALS motor neurons. Arrows denote the nuclei. Bars = 25μm.

might be impaired in the neurodegenerative process of ALS. Among the genes related to transcriptional regulation, the number of significantly downregulated genes was twofold greater than that of the upregulated ones in ALS motor neurons. These downregulated transcription-related genes were not restricted to genes regulating neuronal differentiation as neuron-specific cellular properties, but also included genes such as RNA polymerase and transcription factors, which regulate general cellular functions. These observations suggest that downregulation of transcriptional activity may be the reflection of motor neuron dysfunction because of a wide range of impairments of cellular maintenance systems.

Interestingly, the expression of dynactin 1, which recently has been identified as a causative gene for human motor neuron disease,[42] was reduced in ALS motor neurons. Some other motor proteins including the kinesin family responsible for antegrade axonal transport and dyneins for retrograde axonal transport were not changed significantly, but the expression levels of MAPs 1A, 4, and tau were decreased, shown by their classification in SOM1 and SOM6. The impairment of axonal transport is thought to be an early event of motor neuron degeneration, and especially the protein levels of MAPs 1A and tau have been reported to decrease early before the onset of symptoms in mutant SOD1 transgenic mice.[43–45] The upregulation of ubiquitin-specific protease 11 (USP11), listed in Tables 2 and 3, also may be related to microtubule abnormality because the RanGTP-associated protein RanBPM, which is required for correct nucleation of microtubules, is the enzymatic substrate for USP11.[46] The present results imply that retrograde axonal transport, especially that associated with dynactin, might be affected even at the terminal stage of ALS and be crucial for motor neurons, although cytoskeletal proteins are the major functional group in the downregulated genes.

As for the death signals and inflammatory factors, we previously have reported that these genes were significantly upregulated in the spinal cord of mutant SOD1 transgenic mice,[15,17] suggesting that these inflammatory and apoptotic death signals play a crucial role in concert with motor neuron degeneration and inflammatory cellular reactions, including microglial activation.[7,47] However, in sporadic ALS spinal cords, the expression profiles of inflammation- and death signal–related genes are somewhat different from those in the Tg mouse model. Death receptor 5 (TNF receptor 10b, TNFR10b), TNF receptor–associated factor 6 (TRAF 6), interleukin-1 receptor antagonist, and ephrin A1 were overexpressed in ALS motor neurons, whereas the expression levels of the respective ligands or inducers, TNF-α, TNF superfamily member 10 (TRAIL) and IL-1β, were not markedly changed in either motor neurons or ventral horn homogenates. Because TNF-α was prominently upregulated in the Tg mouse spinal cords,[17] its almost unchanged expression level in sporadic ALS was a surprising observation. Many other inflammation-related genes were also not significantly upregulated in human ALS spinal cords, in contrast with the findings in animal models. Far less invasion and activation of microglia, a major source of TNF-α, IL-1β, and many other inflammatory factors, were seen in human ALS spinal cords at the terminal autopsy stage as compared with those of Tg mice,[48] which could explain these differences.

Genes related to apoptotic pathways, caspase-1, -3, -9, caspase, and RIP adaptor with death domain (CRADD), were upregulated in ALS motor neurons in SOM analysis (SOM24 and SOM25), and an antiapoptotic factor, NF-κB, was markedly upregulated. Although Bax, a proapoptotic Bcl-2 family member, has been reported to increase in ALS motor neurons,[49,50] and another member, Bak, was underexpressed in this study, the expression of Bcl-2 and Bcl-xL, antiapoptotic Bcl-2 family members was not significantly altered in motor neurons, possibly suggesting that Bcl-2 family members are not primarily involved in motor neuron degeneration in sporadic ALS. Cyclin A1 and C were upregulated (SOM25) and cyclin E was downregulated (SOM1) in ALS motor neurons. These cell cycle regulators are specific to G1/S phase transition, and upregulation of these cyclins enhances arrest in G1/S phase, preventing entry into S phase. Our finding on cyclin expression support the recently reported view that G1/S phase is aberrantly activated in ALS motor neurons, eventually inducing motor neuron death.[51] The subcellular localization of cyclin C in the nucleus may trigger cell death signaling mechanisms. These factors related to the cell death signaling pathway, TNFR, TRAF6, CRADD, caspases, cyclins, Bak, and NF-κB may be involved in the motor neuron degeneration process in sporadic ALS, although we cannot simply state that an apoptotic process is present in ALS motor neurons, as has been suggested by many histological analyses.[6] Becausse neuronal cell degeneration and the eventual neuronal cell death process are the results of interactions of complex pathways involving many factors and signaling molecules, we need to further elucidate the pathophysiological significance of these factors with altered expression levels in ALS motor neurons.

Microarray analysis on the laser-captured motor neurons provided us with significant information about motor neuron degeneration and dysfunction in sporadic ALS patients. Such information cannot be obtained by whole spinal cord tissue microarray assay,[52] as discussed above. Although this study was performed on postmortem patients' tissues, the remaining individual motor neurons would express ongoing or even early molecular events in the neurodegeneration process, because motor neurons in the remaining motor neuron population randomly enter into the degeneration process among up to the terminal stage in ALS.[53] We need to study larger numbers of ALS patients, and to understand the pathophysiological roles of candidate genes identified by the combined methodology of DNA microarray analysis and LCM, compared with other neurodegeneration processes. This methodology provides crucial clues about candidate genes whose related products might hamper the disease process of ALS.

This work was supported by a Center of Excellence grant from the Ministry of Education, Culture, Sports, Science and Technology of Japan, and grants from the Ministry of Health, Labor and Welfare of Japan.

References

1. Ince PG, Lowe J, Shaw PJ. Amyotrophic lateral sclerosis: current issues in classification, pathogenesis and molecular pathology. Neuropathol Appl Neurobiol 1998;24:104–117.
2. Bunina TL. On intracellular inclusions in familial amyotrophic lateral sclerosis. Korsakov J Neuropath Psychiat 1962;62: 1293–1296.
3. Okamoto K, Hirai S, Amari M, et al. Bunina bodies in amyotrophic lateral sclerosi immunostained with rabbit anti-cystatin C serum. Neurosci Lett 1993;162:125–128.
4. Cleveland DW, Rothstein JD. From Charcot to Lou Gehrig: deciphering selective motor neuron death in ALS. Nat Rev Neurosci 2001;2:806–819.
5. Bergeron C. Oxidative stress: its role in the pathogenesis of amyotrophic lateral sclerosis. J Neurol Sci 1995;129(suppl): 81–84.
6. Sathasivam S, Ince PG, Shaw PJ. Apoptosis in amyotrophic lateral sclerosis: a review of the evidence. Neuropathol Appl Neurobiol 2001;27:257–274.
7. Hand CK, Rouleau GA. Familial amyotrophic lateral sclerosis. Muscle Nerve 2002;25:135–159.
8. Ishigaki S, Liang Y, Yamamoto M, et al. X-Linked inhibitor of apoptosis protein is involved in mutant SOD1-mediated neuronal degeneration. J Neurochem 2002;82:576–584.

9. Kawahara Y, Ito K, Sun H, et al. Glutamate receptors: RNA editing and death of motor neurons. Nature 2004;427:801.
10. Niwa J, Ishigaki S, Hishikawa N, et al. Dorfin ubiquitylates mutant SOD1 and prevents mutant SOD1-mediated neurotoxicity. J Biol Chem 2002;277:36793–36798.
11. Hishikawa N, Niwa J, Doyu M, et al. Dorfin localizes to the ubiquitylated inclusions in Parkinson's disease, dementia with Lewy bodies, multiple system atrophy, and amyotrophic lateral sclerosis. Am J Pathol 2003;163:609–619.
12. Luo J, Isaacs WB, Trent JM, Duggan DJ. Looking beyond morphology: cancer gene expression profiling using DNA microarrays. Cancer Invest 2003;21:937–949.
13. Alizadeh AA, Ross DT, Perou CM, van de Rijn M. Towards a novel classification of human malignancies based on gene expression patterns. J Pathol 2001;195:41–52.
14. Luo L, Salunga RC, Guo H, et al. Gene expression profiles of laser-captured adjacent neuronal subtypes. Nat Med 1999;5: 117–122.
15. Ando Y, Liang Y, Ishigaki S, et al. Caspase-1 and -3 mRNAs are differentially upregulated in motor neurons and glial cells in mutant SOD1 transgenic mouse spinal cord: a study using laser microdissection and real-time RT-PCR. Neurochem Res 2003; 28:839–846.
16. Ginsberg SD, Hemby SE, Lee VM, et al. Expression profile of transcripts in Alzheimer's disease tangle-bearing CA1 neurons. Ann Neurol 2000;48:77–87.
17. Yoshihara T, Ishigaki S, Yamamoto M, et al. Differential expression of inflammation- and apoptosis-related genes in spinal cords of a mutant SOD1 transgenic mouse model of familial amyotrophic lateral sclerosis. J Neurochem 2002;80:158–167.
18. Kamme F, Salunga R, Yu J, et al. Single-cell microarray analysis in hippocampus CA1: demonstration and validation of cellular heterogeneity. J Neurosci 2003;23:3607–3615.
19. Terao S, Sobue G, Hashizume Y, et al. Disease-specific patterns of neuronal loss in the spinal ventral horn in amyotrophic lateral sclerosis, multiple system atrophy and X-linked recessive bulbospinal neuronopathy, with special reference to the loss of small neurons in the intermediate zone. J Neurol 1994;241: 196–203.
20. Sobue G, Hashizume Y, Yasuda T, et al. Phosphorylated high molecular weight neurofilament protein in lower motor neurons in amyotrophic lateral sclerosis and other neurodegenerative diseases involving ventral horn cells. Acta Neuropathol (Berl) 1990;79:402–408.
21. Bohm M, Wieland I, Schutze K, Rubben H. Microbeam MOMeNT: non-contact laser microdissection of membrane-mounted native tissue. Am J Pathol 1997;151:63–67.
22. Watanabe H, Tanaka F, Doyu M, et al. Differential somatic CAG repeat instability in variable brain cell lineage in dentatorubral pallidoluysian atrophy (DRPLA): a laser-captured microdissection (LCM)-based analysis. Hum Genet 2000;107: 452–457.
23. Schutze K, Lahr G. Identification of expressed genes by laser-mediated manipulation of single cells. Nat Biotechnol 1998;16: 737–742.
24. Wang J, Delabie J, Aasheim H, et al. Clustering of the SOM easily reveals distinct gene expression patterns: results of a reanalysis of lymphoma study. BMC Bioinformatics 2002;3: 36–44.
25. Ross ME, Zhou X, Song G, et al. Classification of pediatric acute lymphoblastic leukemia by gene expression profiling. Blood 2003;102:2951–2959.
26. Malaspina A, Kaushik N, de Belleroche J. Differential expression of 14 genes in amyotrophic lateral sclerosis spinal cord detected using gridded cDNA arrays. J Neurochem 2001;77: 132–145.
27. Dangond F, Hwang D, Camelo S, et al. The molecular signature of late-stage human ALS revelated by expression profiling of post-mortem spinal cord gray matter. Physiol Genomics 2004;16:229–239.
28. Kanamori A, Nakayama J, Fukuda MN, et al. Expression cloning and characterization of a cDNA encoding a novel membrane protein required for the formation of *O*-acetylated ganglioside: a putative acetyl-CoA transporter. Pro Natl Acad Sci USA 1997;94:2897–2902.
29. Malisan F, Franchi L, Tomassini B, et al. Acetylation suppresses the proapoptotic activity of GD3 ganglioside. J Exp Med 2002; 196:1535–1541.
30. Rapport MM, Donnenfeld H, Brunner W, et al. Ganglioside patterns in amyotrophic lateral sclerosis brain regions. Ann Neuol 1985;18:60–67.
31. Chen HH, Tourtellotte WG, Frank E. Muscle spindle-derived neurotrophin 3 regulates synaptic connectivity between muscle sensory and motor neurons. J Neurosci 2002;22:3512–3519.
32. Mears SC, Frank E. Formation of specific monosynaptic connections between muscle spindle afferents and motoneurons in the mouse. J Neurosci 1997;17:3138–3135.
33. Yamamoto M, Sobue G, Yamamoto K, et al. Expression of glial cell line-derived neurotrophic factor mRNA in the spinal cord and muscle in amyotrophic lateral sclerosis. Neurosci Lett 1996; 204:117–120.
34. Zhou H, Muramatsu T, Halfter W, et al. A role of midkine in the development of the neuromuscular junction. Mol Cell Neurosci 1997;10:56–70.
35. Oosthuyse B, Moons L, Storkebaum E, et al. Deletion of the hypoxia-response element in the vascular endothelial growth factor promoter causes motor neuron degeneration. Nat Genet 2001;28:131–138.
36. Lambrechts D, Storkebaum E, Morimoto M, et al. VEGF is a modifier of amyotrophic lateral sclerosis in mice and humans and protects motoneurons against ischemic death. Nat Genet 2003;34:383–394.
37. Gros-Louis F, Laurent S, Lopes AA, et al. Absence of mutations in the hypoxia response element of VEGF in ALS. Muscle Nerve 2003;28:774–775.
38. Kawahara Y, Ito K, Sun H, et al. Low editing efficiency of GluR2 mRNA is associated with a low relative abundance of ADAR2 mRNA in white matter of normal human brain. Eur J Neurosci 2003;18:23–33.
39. Venter JC, Adams MD, Myers EW, et al. The sequence of the human genome. Science 2001;291:1304–1351.
40. Colbert MC, Rubin WW, Linney E, LaMantia AS. Retinoid signaling and the generation of cellular diversity in the embryonic mouse spinal cord. Dev Dyn 1995;204:1–12.
41. Sakakibara S, Okano H. Expression of neural RNA-binding proteins in the postnatal CNS: implications of their roles in neuronal and glial cell development. J Neurosci 1997;17: 8300–8312.
42. Puls I, Jonnakuty C, LaMonte BH, et al. Mutant dynactin in motor neuron disease. Nat Genet 2003;33:455–456.
43. Williamson TL, Cleveland DW. Slowing of axonal transport is a very early event in the toxicity of ALS-linked SOD1 mutants to motor neurons. Nat Neurosci 1999;2:50–56.
44. Zhang B, Tu P, Abtahian F, et al. Neurofilaments and orthograde transport are reduced in ventral root axons of transgenic mice that express human SOD1 with a G93A mutation. J Cell Biol 1997;139:1307–1315.
45. Farah CA, Nguyen MD, Julien JP, Leclerc N. Altered levels and distribution of microtuble-associated protein before disease onset in a mouse model of amyotrophic lateral sclerosis. J Neurochem 2003;84:77–86.

46. Ideguchi H, Ueda A, Tanaka M, et al. Structural and functional characterization of the USP11 deubiquitinating enzyme, which interacts with the RanGTP-associated protein RanBPM. Biochem J 2002;367:87–95.
47. Hensley K, Floyd RA, Gordon B, et al. Temporal patterns of cytokines and apoptosis-related gene expression in spinal cords of the G93A-SOD1 mouse model of amyotrophic lateral sclerosis. J Neurochem 2002;82:365–374.
48. Hall ED, Oostveen JA, Gurney ME. Relationship of microglial and astrocytic activation to disease onset and progression in a transgenic model of familial ALS. Glia 1998;23:249–256.
49. Mu X, He J, Anderson DW, et al. Altered expression of bcl-2 and bax mRNA in amyotrophic lateral sclerosis spinal cord motor neurons. Ann Neurol 1996;40:379–386.
50. Ekegren T, Grundstrom E, Lindholm D, Aquilonius SM. Up-regulation of Bax protein and increased DNA degradation in ALS spinal cord motor neurons. Acta Neurol Scand 1999;100: 317–321.
51. Ranganathan S, Bowser R. Alterations in G(1) to S phase cell-cycle regulators during amyotrophic lateral sclerosis. Am J Pathol 2003;162:823–835.
52. Malaspina A, de Belleroche J. Spinal cord molecular profiling provides a better understanding of amyotrophic lateral sclerosis pathogenesis. Brain Res Brain Res Rev 2004;45:213–229.
53. Sobue G, Sahashi K, Takahashi A, et al. Degenerating compartment and functioning compartment of motor neurons in ALS: possible process of motor neuron loss. Neurology 1983;33: 654–657.

doi:10.1093/brain/awh381 *Brain* (2005), **128**, 659–670

Widespread nuclear and cytoplasmic accumulation of mutant androgen receptor in SBMA patients

Hiroaki Adachi,[1] Masahisa Katsuno,[1] Makoto Minamiyama,[1] Masahiro Waza,[1] Chen Sang,[1] Yuji Nakagomi,[2] Yasushi Kobayashi,[1] Fumiaki Tanaka,[1] Manabu Doyu,[1] Akira Inukai,[1] Mari Yoshida,[3] Yoshio Hashizume[3] and Gen Sobue[1]

[1]*Department of Neurology, Nagoya University Graduate School of Medicine, Nagoya,* [2]*Central Research Laboratories, School of Medicine, Aichi Medical University and* [3]*Department of Neuropathology, Institute for Medical Sciences of Aging, Aichi Medical University of Aichi, Japan*

Correspondence to: Gen Sobue, MD, PhD, Department of Neurology, Nagoya University Graduate School of Medicine, 65 Tsurumai-cho Showa-ku, Nagoya, 466-8550, Japan
E-mail: sobueg@med.nagoya-u.ac.jp

Summary

Spinal and bulbar muscular atrophy (SBMA) is an inherited adult onset motor neuron disease caused by the expansion of a polyglutamine (polyQ) tract within the androgen receptor (AR), affecting only males. The characteristic pathological finding is nuclear inclusions (NIs) consisting of mutant AR with an expanded polyQ in residual motor neurons, and in certain visceral organs. We immunohistochemically examined 11 SBMA patients at autopsy with 1C2, an antibody that specifically recognizes expanded polyQ. Our study demonstrated that diffuse nuclear accumulation of mutant AR was far more frequent and extensive than NIs being distributed in a wide array of CNS nuclei, and in more visceral organs than thus far believed. Mutant AR accumulation was also present in the cytoplasm, particularly in the Golgi apparatus; nuclear or cytoplasmic predominance of accumulation was tissue specific. Furthermore, the extent of diffuse nuclear accumulation of mutant AR in motor and sensory neurons of the spinal cord was closely related to CAG repeat length. Thus, diffuse nuclear accumulation of mutant AR apparently is a cardinal pathogenetic process underlying neurological manifestations, as in SBMA transgenic mice, while cytoplasmic accumulation may also contribute to SBMA pathophysiology.

Keywords: polyglutamine; spinal and bulbar muscular atrophy; diffuse nuclear accumulation; nuclear inclusion, cytoplasmic accumulation

Abbreviations: polyQ = polyglutamine; SBMA = spinal and bulbar muscular atrophy; AR = androgen receptor; NIs = nuclear inclusions; DRPLA = dentatorubral-pallidoluysian atrophy; CBP = CREB-binding protein

Received June 15, 2004. First revision August 23, 2004. Second revision November 26, 2004. Accepted November 30, 2004. Advance Access publication January 19, 2005

Introduction

Polyglutamine (polyQ) diseases are inherited neurodegenerative disorders caused by expansion of a trinucleotide CAG repeat in the causative genes. To date, nine polyQ diseases have been identified (Ross, 2002). Spinal and bulbar muscular atrophy (SBMA) is a polyQ disease involving mainly spinal and brainstem motor neurons (Kennedy *et al.*, 1968; Sobue *et al.*, 1989). In SBMA, a polymorphic CAG repeat ordinarily consisting of 14–32 CAGs is expanded to 40–62 CAGs in the first exon of the androgen receptor (AR) gene (La Spada *et al.*, 1991; Tanaka *et al.*, 1996), and shows somatic mosaicism (Tanaka *et al.*, 1999). An inverse correlation exists between CAG repeat size and age at onset as well as disease severity in SBMA (Doyu *et al.*, 1992; Igarashi *et al.*, 1992; La Spada *et al.*, 1992). SBMA patients develop premature muscular exhaustion, and subsequently slowly progressive muscular weakness, atrophy and fasciculations in bulbar and limb muscles (Kennedy *et al.*, 1968; Sobue *et al.*, 1989; Sperfeld *et al.*, 2002). SBMA patients may also have mild sensory impairment, which usually remains subclinical (Sobue *et al.*, 1989; Li *et al.*, 1995; Mariotti *et al.*, 2000). Besides these symptoms of neuronal degeneration, androgen insensitivity symptoms such as gynaecomastia, testicular atrophy and reduced fertility are common (Arbizu *et al.*, 1983). Elevated serum creatine kinase concentrations, impaired glucose tolerance, hepatic dysfunction and hyperlipidaemia are frequent (Sobue *et al.*, 1989; Li *et al.*, 1995). These findings show that involvement of

SBMA is not restricted to motor neurons, but extends to several visceral organs.

The cardinal pathological findings of SBMA are motor neuron loss in the spinal cord and brainstem (Sobue *et al.*, 1989) and the presence of the nuclear inclusions (NIs), representing mutant AR, in residual motor neurons in brainstem motor nuclei, in spinal motor neurons (Li *et al.*, 1998*a*) and in certain visceral organs (Li *et al.*, 1998*b*). However, diffuse nuclear accumulation of the mutant protein has been detected in a more widespread distribution than NIs in a transgenic mouse model of SBMA (Katsuno *et al.*, 2002, 2003; Adachi *et al.*, 2003) and in models of other polyQ diseases (Schilling *et al.*, 1999; Yvert *et al.*, 2000; Lin *et al.*, 2001). Such accumulation has been found to be relevant to neuronal dysfunction and eventual symptom appearance. Indeed, in dentatorubral-pallidoluysian atrophy (DRPLA), tissue distribution of diffuse nuclear accumulation of the responsible mutant protein was more widespread and more relevant to the disease severity and symptoms than that of NIs (Yamada *et al.*, 2001*a*, *b*).

Recently we demonstrated in our transgenic mouse model that diffuse nuclear mutant AR accumulation can be prevented by reduction of circulating testosterone with castration or with an anti-androgenic agent such as leuprolerin; in treated animals, motor function and survival rate were dramatically improved (Katsuno *et al.*, 2002, 2003), suggesting that disease manifestation in SBMA is highly testosterone dependent (Lieberman *et al.*, 2002; Walcott and Merry, 2002*a*; Chevalier-Larsen *et al.*, 2004). Indeed, a female carrier of SBMA, even if homozygous, does not express disease phenotypes (Sobue *et al.*, 1993; Schmidt *et al.*, 2002), presumably because circulating testosterone concentrations are low. These observations indicate that nuclear translocation and nuclear accumulation of mutant AR, detected as diffuse nuclear accumulation, is closely linked to the phenotypic expressions and that diffuse nuclear mutant AR accumulation is of major pathogenetic importance in neuronal dysfunction (Katsuno *et al.*, 2002, 2003).

In this study, to understand better the pathophysiology of SBMA, we examined neural and non-neural tissue distributions of mutant AR accumulation in 11 SBMA patients at autopsy, using 1C2, an antibody specific for the expanded polyQ tract, as well as antibodies against AR. First, diffuse nuclear accumulation of mutant AR was far more extensive than that of NIs. Secondly, mutant AR accumulation was also present in cytoplasm, specifically in the Golgi apparatus, with predominance of nuclear or cytoplasmic accumulation being tissue specific. Thirdly, the extent of diffuse nuclear accumulation was closely related to CAG repeat length. Our present results strongly suggested that diffuse nuclear accumulation of mutant AR is of critical pathogenetic importance for motor symptoms as in the SBMA transgenic mouse model, although cytoplasmic accumulation may also contribute to the pathophysiology of SBMA.

Subjects and methods

Patients

Eleven patients with clinicopathologically and genetically confirmed SBMA (age at death, 51–84 years; mean, 66) were examined in this study (Table 1). These patients had been hospitalized and followed-up at Nagoya University Hospital and its affiliated hospitals during the past 25 years. Age at onset ranged between 20 and 75 years, and muscle weakness and bulbar symptoms had progressed for 6–53 years. Elevated serum creatine kinase and glucose was observed in many patients. Causes of death included respiratory failure related to pneumonia in seven patients, lung cancer and colon cancer in one patient each, and tuberculosis and suffocation in one patient each. At autopsy, the brain, spinal cord, dorsal root ganglia, thoracic sympathetic ganglia and various visceral organs were removed and fixed in 10% buffered formalin solution. CAG repeat length in the *AR* gene ranged between 40 and 50. Five other subjects (age 60–74 years, mean 67.3) who died of non-neurological diseases served as controls.

Tissue preparation and immunohistochemistry

We prepared 5 μm thick, formalin-fixed, paraffin-embedded sections of various portions of the cerebrum, brainstem, cerebellum,

Table 1 *Clinical features of 11 SBMA patients*

Patient	Age at death (years)	Onset of limb weakness (years)	CK (normal range)	Glucose (mg/dl)	$(CAG)_n$	Cause of death
1	74	20	455 (57–197)	84*	48	Pneumonia
2	60	27	477 (36–203)	276	50	Pneumonia
3	71	50	995 (53–288)	141	48	Pneumonia
4	60	40	191 (32–197)	134	44	Lung cancer
5	78	25	411 (30–170)	362	42	Pneumonia
6	84	75	75 (<110)	100	40	Tuberculosis, silicosis
7	51	41	712 (30–170)	96*	47	Pneumonia
8	66	41	471 (<120)	163	48	Pneumonia
9	72	39	45 (<25)	101*	43	Colon cancer
10	59	53	301 (8–80)	105*	ND	Suffocation
11	51	27	173 (20–100)	101	ND	Pneumonia

CK = serum creatine kinase; $(CAG)_n$ = number of expanded CAG repeats in the AR allele. $(CAG)_n$ was determined on the DNA from blood samples (patients 1–7) or from stored tissue samples (patients 8 and 9, liver). *Impaired glucose tolerance assessed with 75 g oral glucose tolerance test. ND = not determined.

spinal cord, dorsal root ganglia, sympathetic ganglia, pituitary gland, peripheral nerve, muscle and non-neural visceral organs from SBMA and control subjects. Sections then were deparaffinized and rehydrated through a graded series of alcohol–water solutions. For the mutant AR immunohistochemical study, sections were pre-treated with immersion in 98% formic acid for 5 min and then with microwave oven heating for 10 min in 10 mM citrate buffer at pH 6.0. Sections were blocked with normal serum from the animal species in which each second antibody was raised (1 : 20), and then incubated with a mouse anti-expanded polyQ antibody (Trottier *et al.*, 1995) (1C2; Chemicon, Temecula, CA; 1 : 10 000); a mouse anti-Golgi 58K protein antibody (Sigma, St. Louis, MO; 1 : 100); rabbit polyclonal antibody N-20 (Santa Cruz Biotechnology, Santa Cruz, CA; 1 : 200); rabbit polyclonal antibody PG-21 (Affinity BioReagents, Golden, CO; 1 : 200); rabbit polyclonal antibody H-280 (Santa Cruz; 1 : 200); rabbit polyclonal antibody C-19 (Santa Cruz; 1 : 200); or a mouse monoclonal antibody (Ab-1; Neomarkers, Fremont, CA; ready-to-use) against human AR protein. Then the sections were incubated with biotinylated IgG raised against the species used for each primary antibody (Vector Laboratories, Burlingame, CA). Immune complexes were visualized using streptavidin–horseradish peroxidase (Dako, Glostrup, Denmark) and 3,3′-diaminobenzidine (Dojindo, Kumamoto, Japan) substrate. Sections were counterstained with methyl green or Mayer's haematoxylin. As a negative control, primary antibodies were replaced with normal rabbit or mouse serum. The population of labelled neurons was analysed semi-quantitatively in all 11 SBMA patients, and non-neural visceral organs in nine patients (patients 1–8, and 11) by counting the positive and negative cells for labelling in the region of interest and graded as – to +++.

To assess the co-localization of cytoplasmic mutant AR accumulation and cell organelles, five selected SBMA patients (patients 1, 2, 6, 8 and 10) were analysed by double immunofluorescence staining. The sections were blocked with 5% normal serum and then sequentially incubated at 4°C overnight with any antibody to lysosomal markers, anti-cathepsin B antibody (Ab-3; Oncogene, Cambridge, MA; 1 : 20), anti-cathepsin D antibody (Ab-2; Oncogene; 1 : 20), anti-cathepsin K antibody (N-20; Santa Cruz Biotechnology; 1 : 50), anti-cathepsin L antibody (S-20; Santa Cruz Biotechnology; 1 : 50), antibody to Golgi apparatus, anti-human TGN46 antibody (Serotec, Oxford, UK; 1 : 1000), antibody to endoplasmic reticulum marker, anti-GRP78 antibody (N-20; Santa Cruz; 1 : 200), or antibody to mitochondria, anti-mitochondria antibody (Chemicon; 1 : 50), and 1C2 antibody (Chemicon; 1 : 10 000). Sections were incubated with Alexa 488-conjugated anti-mouse IgG (Molecular Probes, Leiden, The Netherlands; 1 : 1300) and Alexa 568-conjugated IgG raised against the species used for each primary antibody (Molecular Probes; 1 : 1000). For double immunofluorescence staining using anti-human TGN46 antibody, sections were incubated with biotinylated anti-sheep IgG (Vector Laboratories; 1 : 400) for 8 h at 4°C, the sections were incubated with Alexa 568-conjugated streptavidin (Molecular Probes; 1 : 1000) and Alexa 488-conjugated anti-mouse IgG (Molecular Probes; 1 : 1300) for 2 h at 4°C. Sections then were examined and photographed using a confocal laser scanning microscope (MRC 1024; Bio-Rad Laboratories, Hercules, CA).

For electron microscopic immunohistochemistry, buffered formalin-fixed, paraffin-embedded tissue sections were deparaffinized, rehydrated, immunostained with 1C2 antibody (Chemicon, 1 : 10 000), and then incubated with biotinylated anti-mouse IgG (Vector Laboratories; 1 : 1300). Immunoreactivity in tissue sections was visualized using streptavidin–horseradish peroxidase (Dako) and 3,3′-diaminobenzidine substrate (Dojindo), fixed with 2% osmium tetroxide in 0.1 mol/l phosphate buffer at pH 7.4, dehydrated in graded alcohol–water solutions, and embedded in epoxy resin. Ultrathin sections then were cut for observation under an electron microscope (H-7100; Hitachi High-Technologies Corporation, Tokyo, Japan).

Quantification of diffuse nuclear- and NI-positive cell populations

For quantitative assessment, we prepared at least 100 transverse sections each from the cervical, thoracic and lumbar spinal cord for staining with 1C2 antibody as above. The numbers of 1C2-positive and -negative cells in the ventral and dorsal horn on both right and left sides were counted on every 10th section under the light microscope with a computer-assisted image analyser (Luzex FS; Nikon, Tokyo, Japan). For the purposes of counting, a cell was defined by the presence of its nucleus in a given 5 μm thick section. Diffuse nuclear staining and NI-positive neurons were assessed separately. Neurons showing both diffuse nuclear staining and NIs were counted in both categories. The area of the ventral and dorsal horn of each spinal cord section was determined as described previously (Terao *et al.*, 1996; Adachi *et al.*, 2001). Populations of 1C2-positive cells were expressed as percentages of the total neuronal count. For statistical analysis, mean values of these percentages in sections examined from each of the cervical, thoracic and lumbar spinal segments for each patient were obtained.

Statistical analysis

We analysed the data by Pearson's correlation coefficient and Spearman's rank correlation as appropriate using Statview software (version 5; Hulinks, Tokyo, Japan), considering P values <0.05 to be indicative of significance.

Results

Immunohistochemical localization of mutant androgen receptor in the neural tissues

In all 11 patients with SBMA, NIs were visualized clearly with 1C2 (Fig. 1). In addition to NIs, diffusely distributed staining with 1C2 was observed in neuronal nuclei (Fig. 1). Among nuclei with diffuse staining, some showed punctate, granular or web-like patterns, while others showed intense diffuse staining (Fig. 1). In some neurons, NIs and diffuse nuclear staining co-existed (Fig. 1). Moreover, occasional neurons showed granular or punctate 1C2-positive accumulation in the cytoplasm (Fig. 1). As reported previously (Li *et al.*, 1998*a*, *b*), NIs were observed frequently in lower motor neurons, which are known to be affected in this disease. However, we found that neuronal nuclear and cytoplasmic accumulations extended to various regions of the nervous system previously reported to be spared (Li *et al.*, 1998*a*, *b*), including the striatum, caudate nucleus, mammillary body, thalamus, hypothalamus, reticular formation, red nucleus, substantia nigra, locus coerulus, nucleus raphe pontis, pontine nuclei, cuneate nucleus, nucleus ambiguus, gracile nucleus, supraspinal nucleus, cerebellar dentate nucleus, Clarke's

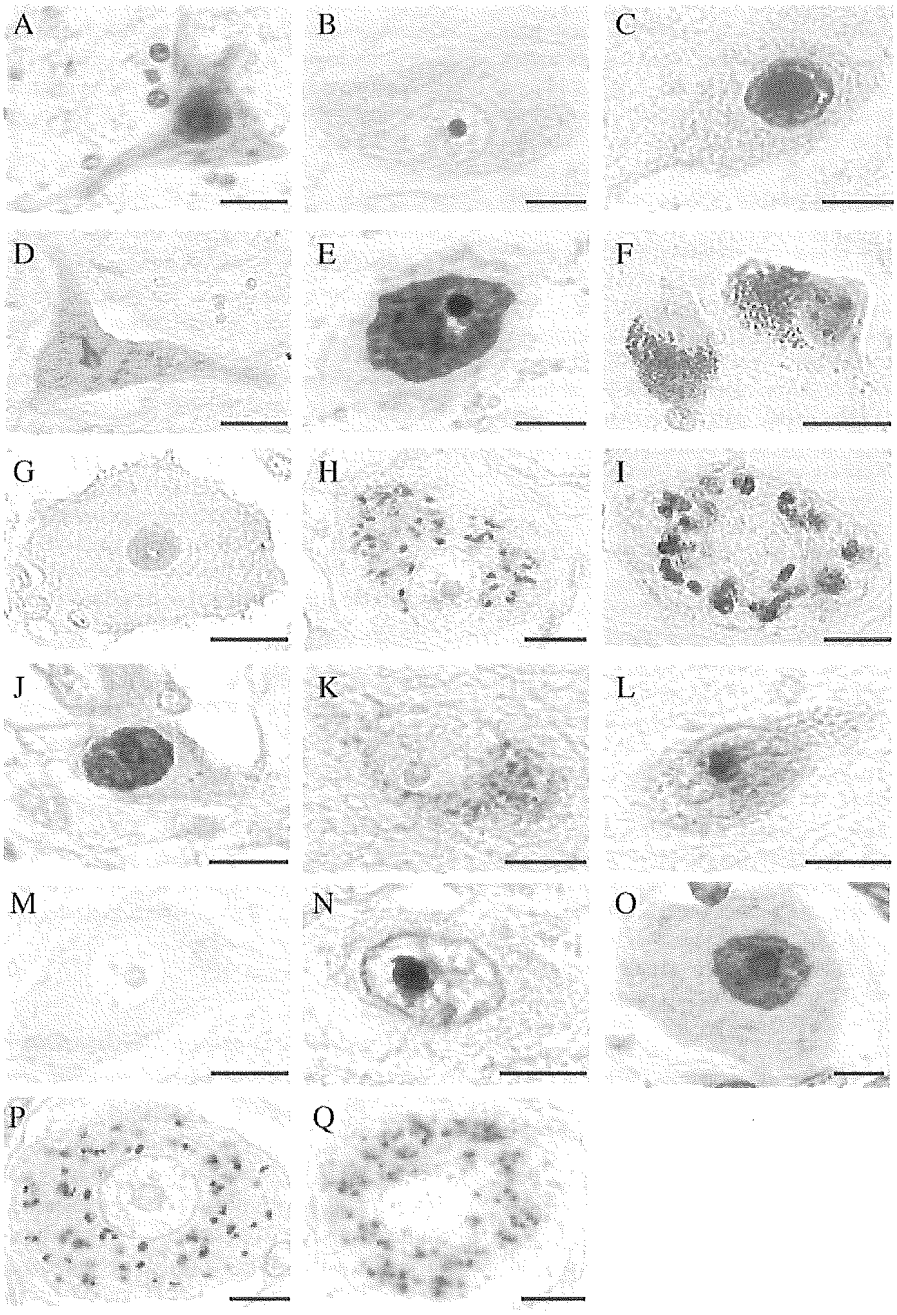

Fig. 1 Immunohistochemical analysis in the neural tissues from SBMA patients and control cases. In the CNS of SBMA patients, intense diffuse nuclear staining is present in neuronal nuclei of various regions using 1C2 antibody (**A**, **E**, **F**, **G**, **J** and **L**). Diffuse immunostaining of mutant androgen receptor (AR) is present in a web-like pattern in nuclei of anterior horn neurons (**A**). Diffuse nuclear staining is also observed in posterior horn neurons (**E**), substantia nigra (**F**), spinal dorsal root ganglia (**G**), paravertebral sympathetic ganglia (**J**) and hypothalamus (**L**). Some nuclei appear packed with mutant AR. Small or large nuclear inclusions are also stained intensely using 1C2 antibody in anterior horn neurons (**B–D**), posterior horn neurons (**E**), the substantia nigra (**F**) and the hypothalamus (**L**). Most of the dark brown pigment seen in the neuronal cytoplasm in the substantia nigra (**F**) is neuromelanin. In addition to nuclear inclusions, occasional neurons exhibit granular structures immunoreactive for 1C2 in the cytoplasm, such as in the anterior horn (**D**) and hypothalamus (**K**). In spinal dorsal root ganglia, small or large cytoplasmic inclusions are frequent (**H** and **I**). There is no immunoreactivity for 1C2 in the spinal anterior horn cell from the control case (**M**). Immunopositive nuclear inclusions and diffuse nuclear staining are also present using H280 antibody in the spinal anterior horn cell (**N**) and spinal dorsal root ganglia (**O**). Spinal dorsal root ganglia neurons exhibit granular structures immunoreactive for anti-Golgi 58K protein antibody in the cytoplasm in SBMA (**P**) and a control case (**Q**). Scale bars = 20 μm for **A**, **D**, **F**, **G**, **M** and **O**; and 10 μm for **B**, **C**, **E**, **H**, **I**, **J**, **K**, **L**, **N**, **P** and **Q**.

nucleus, posterior horn and intermediolateral nucleus of the spinal cord, dorsal root ganglia and sympathetic ganglia (Fig. 1, Table 2). Cytoplasmic inclusions were prominent in the dorsal root ganglia neurons, and some neurons in the mammillary body, hypothalamus and facial motor nucleus and anterior and posterior horns of the spinal cord showed a slight degree of cytoplasmic accumulation (Table 2). We detected both nuclear and cytoplasmic accumulations in some neurons (Fig. 1D). No significant difference in staining pattern was evident between regions previously reported to be affected and unaffected. Diffuse nuclear staining was seen more frequently than NIs in most regions (Table 2). Relative numbers of stained neurons varied between patients, but no staining was detected in cerebral cortex, hippocampus or cerebellar cortex. In contrast to neurons, NIs and diffuse nuclear staining were very rare in glial cells. NIs stained strongly with anti-ubiquitin antibody, while cytoplasmic accumulations did not (data not shown). Anti-human AR antibodies also recognized NIs (Fig. 1N), and occasionally stained diffuse nuclear accumulations (Fig. 1O). However, cytoplasmic accumulations were not seen with anti-AR antibodies.

Table 2 *Immunohistochemical distribution of mutant AR in the neural tissues of patients with SBMA*

Region	Nuclear accumulation		Cytoplasmic accumulation
	Diffuse nuclear accumulation	NI	
Cerebrum			
Cerebral cortex	−	−	−
Striatum	+	+	−
Caudate nucleus	+	+	−
Mammillary body	−	−	+
Thalamic nuclei	+	+	−
Hypothalamus	+ to ++	+	+
Midbrain			
Superior colliculus	−	−	−
Periaqueductal grey	+	+	−
Oculomotor nucleus	−	−	−
Reticular formation of midbrain	+	+	−
Red nucleus	+	+	−
Substantia nigra	+	+	−
Pons			
Locus coerulus	+	+	−
Trigeminal motor nucleus	+ to ++	+	−
Reticular formation of pons	+	+	−
Facial motor nucleus	+ to +++	+	+
Nucleus raphe pontis	+	+	−
Pontine nuclei	+	+	−
Medulla			
Cuneate nucleus	+	+	−
Hypoglossal nucleus	+ to ++	+	−
Nucleus ambiguus	+ to ++	+	−
Gracile nucleus	+	+	−
Supraspinal nucleus	+ to ++	+	−
Accessory nucleus	+	+	−
Cerebellum			
Purkinje cell	−	−	−
Granule cell	−	−	−
Cerebellar dentate nucleus	+	+	−
Spinal cord			
Anterior horn motor neurons	+ to +++	+ to ++	+
Intermediate zone	+	+	−
Clarke's nucleus	+	−	−
Posterior horn neurons	+ to ++	− to +	+
Intermediolateral nucleus	+	+	
Dorsal root ganglia	+	+	++ to +++
Sympathetic ganglia	+	+	−

Frequency of neurons expressing polyglutamine immunoreactivity: −, 0%; +, 0–4%; ++, 4–8%; +++, 8%.

Electron microscopic immunohistochemistry for 1C2 demonstrated granular dense aggregates without a limiting membrane corresponding to NIs and cytoplasmic accumulations, whereas amorphous aggregates corresponded to diffuse nuclear staining in neurons (Fig. 2). No filamentous structures such as those reported in Huntington's disease, DRPLA and Machado–Joseph disease were seen. Neural tissues from five control cases were also examined in the same manner as that for SBMA cases; in these, NIs, diffuse nuclear staining and cytoplasmic accumulations were not seen, indicating that the immunohistochemical procedure with the highly diluted condition of 1C2 applied in this study did not recognize the TATA-binding protein, a transcription factor containing a stretch of polyQ residues (Trottier *et al.*, 1995), as previously demonstrated (Yamada *et al.*, 2001*a*, 2002*a*).

Although we did not quantitatively examine neuronal populations in this study, the motor neurons in the spinal cord and brainstem showed the most conspicuous depletion, as expected. Neurons in the posterior horn of the spinal cord, where diffuse nuclear accumulations and NIs were present in relatively high frequency, also appeared to be depleted to some extent. Quantitative assessment of neuronal cell populations in regions newly showing mutant AR accumulation will be needed.

Co-localization of cytoplasmic organelles with mutant AR

We performed immunofluorescence with double staining using primary antibodies to recognize specifically various cytoplasmic cell organelles together with 1C2 in the dorsal root ganglia, where cytoplasmic mutant AR accumulation was most prominent (Table 2). TGN46 and 1C2 were co-localized (Fig. 3), indicating that mutant AR exists in the Golgi apparatus. Spinal dorsal root ganglia neurons exhibit some granular structures immunoreactive for another Golgi apparatus marker anti-Golgi 58K protein antibody in the cytoplasm (Fig. 1P and Q). Other organelle markers, including antibodies for lysosomes, endoplasmic reticulum and mitochondria, did not show co-localization with 1C2 (Fig. 3), indicating that expanded polyQ sequences were not detected in these organelles.

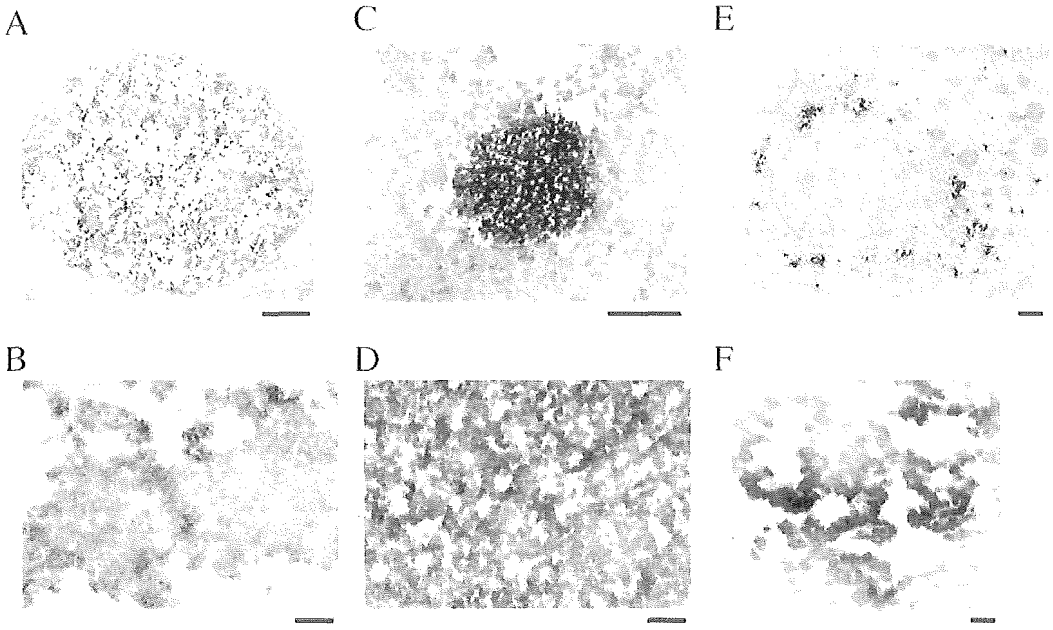

Fig. 2 Electron microscopic immunohistochemical study of nuclear inclusions in motor neurons, and of diffuse nuclear staining and cytoplasmic inclusions in sensory neurons. Electron microscopic immunohistochemistry using 1C2 demonstrated amorphous aggregates corresponding to diffuse nuclear staining in the spinal dorsal root ganglia (**A** and **B**), and granular dense aggregates without fibrous configurations corresponding to nuclear and cytoplasmic inclusions in the spinal anterior neuron (**C** and **D**) and spinal dorsal root ganglia (**E** and **F**). Scale bars = 2 μm for **A**, **C** and **E**; and 200 nm for **B**, **D** and **F**.

Correlation of diffuse nuclear accumulation and NIs with degree of CAG repeat expansion

We examined the correlation of diffuse nuclear accumulation and NIs with the degree of CAG repeat expansion in anterior and posterior horn spinal cord neurons. Averaged frequencies of diffuse nuclear accumulations and NIs in cervical, thoracic and lumbar spinal segments were evaluated for correlation with numbers of CAG repeats in the *AR* gene. The frequency of diffuse nuclear accumulation in anterior and posterior horn neurons correlated well with the degree of CAG repeat expansion (Fig. 4; $r = 0.78$, $P < 0.05$ and $r = 0.69$, $P < 0.05$, respectively). However, the frequency of NIs in motor neurons and posterior horn neurons did not show a significant correlation with number of CAG repeats (Fig. 4; $r = 0.05$, P = NS and $r = -0.14$, P = NS, respectively). These observations strongly suggest that diffuse nuclear accumulation of the mutant AR protein is more important pathogenetically than NIs.

Immunohistochemical localization of mutant AR in non-neural tissues

As in neural tissues, diffuse nuclear accumulations, NIs or cytoplasmic accumulations of mutant AR were observed in certain visceral organs and skin (Fig. 5, Table 3). Diffuse nuclear accumulations and NIs were detected in the liver, proximal tubules of the kidney, testis, prostate gland, and scrotal and other skin (Fig. 5, Table 3). Cytoplasmic accumulations were detected in the liver, pancreatic islets of Langerhans, testis and prostate gland (Fig. 5, Table 3). Nuclear labelling and cytoplasmic accumulation both were absent in the pituitary gland, heart, lung, intestine, spleen, thyroid, adrenal gland and skeletal muscles. Pancreatic islet cells showed exclusively cytoplasmic accumulations without detectable nuclear accumulations, suggesting that the impaired glucose tolerance frequently observed in our patients (Table 1) could be attributed to cytoplasmic mutant AR accumulation. Ubiquitin staining detected only NIs and, as observed in neural tissues, anti-human AR antibodies occasionally showed diffuse nuclear accumulation without cytoplasmic staining (Fig. 5J). The five control cases did not show any 1C2 immunoreactivity in viscera or skin.

Discussion

The present study clearly demonstrated that diffuse nuclear accumulation of mutant AR, detected by the antibody 1C2 which specifically recognizes the expanded polyQ tract, occurred more frequently than NIs in neural and non-neural tissues in SBMA patients. In neural tissues, diffuse nuclear mutant AR accumulation occurred in the basal ganglia, thalamus, hypothalamus, various midbrain, pontine and medullary nuclei, posterior horn, intermediolateral and Clarke's nuclei of the spinal cord and in sensory and sympathetic ganglion neurons, as well as brainstem and spinal cord motor neurons. NIs detected by 1C2 were similar

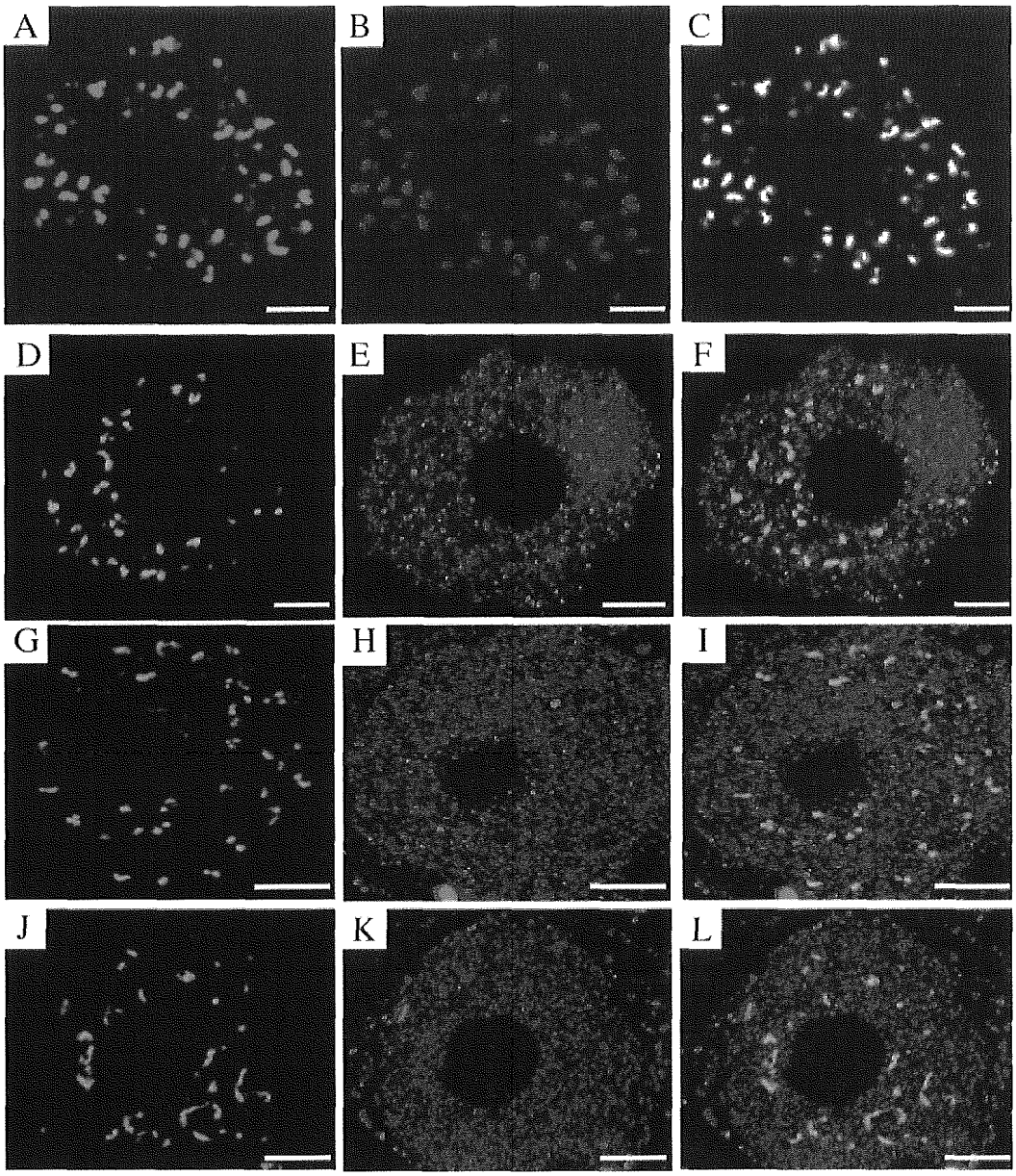

Fig. 3 Co-localization of organelles with mutant AR accumulation. Double immunofluorescence staining with antibodies against TGN46 and expanded polyQ reveals that TGN46 and mutant androgen receptor (AR) are co-localized, as shown for (**A**) expanded polyQ (green), (**B**) TGN46 (red) and (**C**) superimposition of the two signals (yellow) in neurons of the spinal dorsal root ganglia in SBMA, suggesting that mutant AR exists in the Golgi apparatus. Cytoplasmic co-localization of cathepsin B (**E**), GRP78 (**H**) and mitochondria (**K**) with mutant AR (**D**, **G** and **J**) is not observed in dorsal root ganglia (shown in **F**, **I** and **L**), suggesting that the endoplasmic reticulum, lysosomes and mitochondria are unassociated with mutant AR. Scale bars = 10 μm for **A–L**.

in distribution to diffuse nuclear accumulation, but the frequency of NIs in each tissue was far less than for diffuse nuclear accumulation. We previously demonstrated that diffuse nuclear mutant AR protein accumulation was more extensive than NIs in male SBMA transgenic mice (Katsuno *et al.*, 2002, 2003). Furthermore, expression and severity of motor dysfunction, and abatement of abnormalities when the mice were castrated or given leuprolerin, paralleled the extent of diffuse nuclear mutant AR accumulation rather than that of NIs (Katsuno *et al.*, 2002, 2003). Accordingly, neuronal dysfunction appeared to be closely related to diffuse nuclear mutant AR accumulation. The key observation in the present study was a significant close correlation between frequency of diffuse nuclear mutant AR accumulation and length of CAG repeat expansion, while a similar correlation was not observed between frequency of NIs and CAG repeats. Diffuse nuclear

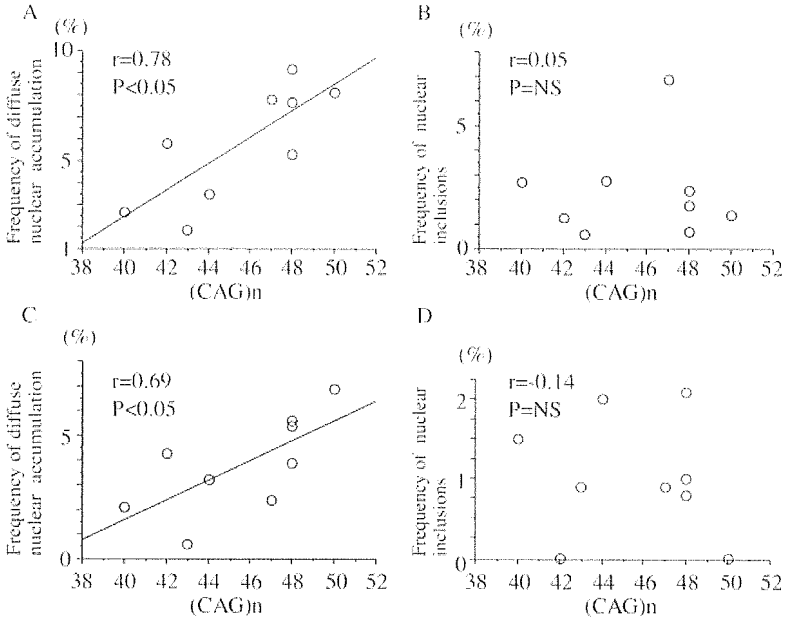

Fig. 4 The relationship of the number of CAG repeats to the frequency of diffuse nuclear accumulation and nuclear inclusions. Diffuse nuclear staining correlates significantly with the number of CAG repeats in anterior horn neurons (**A**) and posterior horn neurons (**C**). On the other hand, nuclear inclusions do not correlate significantly with the number of CAG repeats in the anterior horn neurons (**B**) or posterior horn neurons (**D**).

mutant protein accumulation also has been demonstrated in the neural tissues affected by DRPLA (Yamada *et al.*, 2001*a*, 2002*a*), Huntington's disease (Sapp *et al.*, 1997) and Machado–Joseph disease (Yamada *et al.*, 2001*b*) as well as corresponding transgenic mouse models (Schilling *et al.*, 1999; Yvert *et al.*, 2000; Lin *et al.*, 2001); and, here too, diffuse nuclear mutant protein accumulation was more widespread and extensive than NIs in DRPLA patients. These observations are in good agreement with our present observation in SBMA patients; together, they suggest that diffuse nuclear accumulation of mutant proteins with an expanded polyQ tract is an early event prior to NI formation that is closely related to manifestation of neuronal dysfunction (Yamada *et al.*, 2001*a*; Garden *et al.*, 2002; Katsuno *et al.*, 2002, 2003; Watase *et al.*, 2002; Yoo *et al.*, 2003). However, the molecular pathogenetic process by which diffuse nuclear mutant AR accumulation induces neuronal dysfunction still is unclear. Although considerable controversy recently surrounds the importance of NIs in the pathophysiology in polyQ diseases (Simeoni *et al.*, 2000; Walcott and Merry, 2002*b*; Bates, 2003; Michalik and Van Broeckhoven, 2003; Ross *et al.*, 2003), our data showed that diffuse mutant AR accumulation in nuclei could have potent cytotoxic effects inducing neuronal dysfunction through an active epitope of the expanded polyQ tract.

Anti-AR antibodies showed the ability to detect NIs, and some of them (H280, N-20 and Ab-1) occasionally stained diffuse nuclear accumulations. Diffuse nuclear accumulation had the appearance of amorphous aggregates of mutant AR as observed by electron microscopic immunohistochemistry using 1C2 (Fig. 2) (Katsuno *et al.*, 2002). These observations suggest that the polyQ tract epitope can be detected by 1C2, while other AR protein epitopes may be protected by structural features of the aggregate state of the mutant AR. This view is supported by observations made by small-angle X-ray scattering and infrared spectroscopy carried out with myoglobin protein containing an inserted highly expanded polyQ tract, localizing the polyQ tract to the surface of aggregates, while other epitopes were sequestered within aggregates (Tanaka *et al.*, 2001, 2003). These observations suggest that 1C2 can detect the amorphous aggregate state of mutant AR protein, making 1C2 a more sensitive histological and pathophysiological marker than anti-AR protein antibodies. On the other hand, cytoplasmic accumulations were not seen with anti-AR antibodies. This cytoplasmic mutant AR was not ubiquitinated, in contrast to nuclear accumulated mutant AR, particularly the heavily ubiquitinated NIs, suggesting that protein modification varies between the nucleus and cytoplasm. Different protein modification might mask other AR protein epitopes directly or through structural alterations of the aggregate state of the mutant AR in the cytoplasm.

Another important observation in our study was the occurrence of cytoplasmic mutant AR accumulation in neural and non-neural tissues. In neural tissues, cytoplasmic accumulation was restricted to certain neuronal populations such as dorsal root ganglia neurons, mammillary body, hypothalamus, facial motor nucleus, and anterior and posterior horn neurons. In non-neural tissues, cytoplasmic accumulation also occurred in certain organs. Cytoplasmic mutant AR accumulation co-localized with a Golgi apparatus marker.

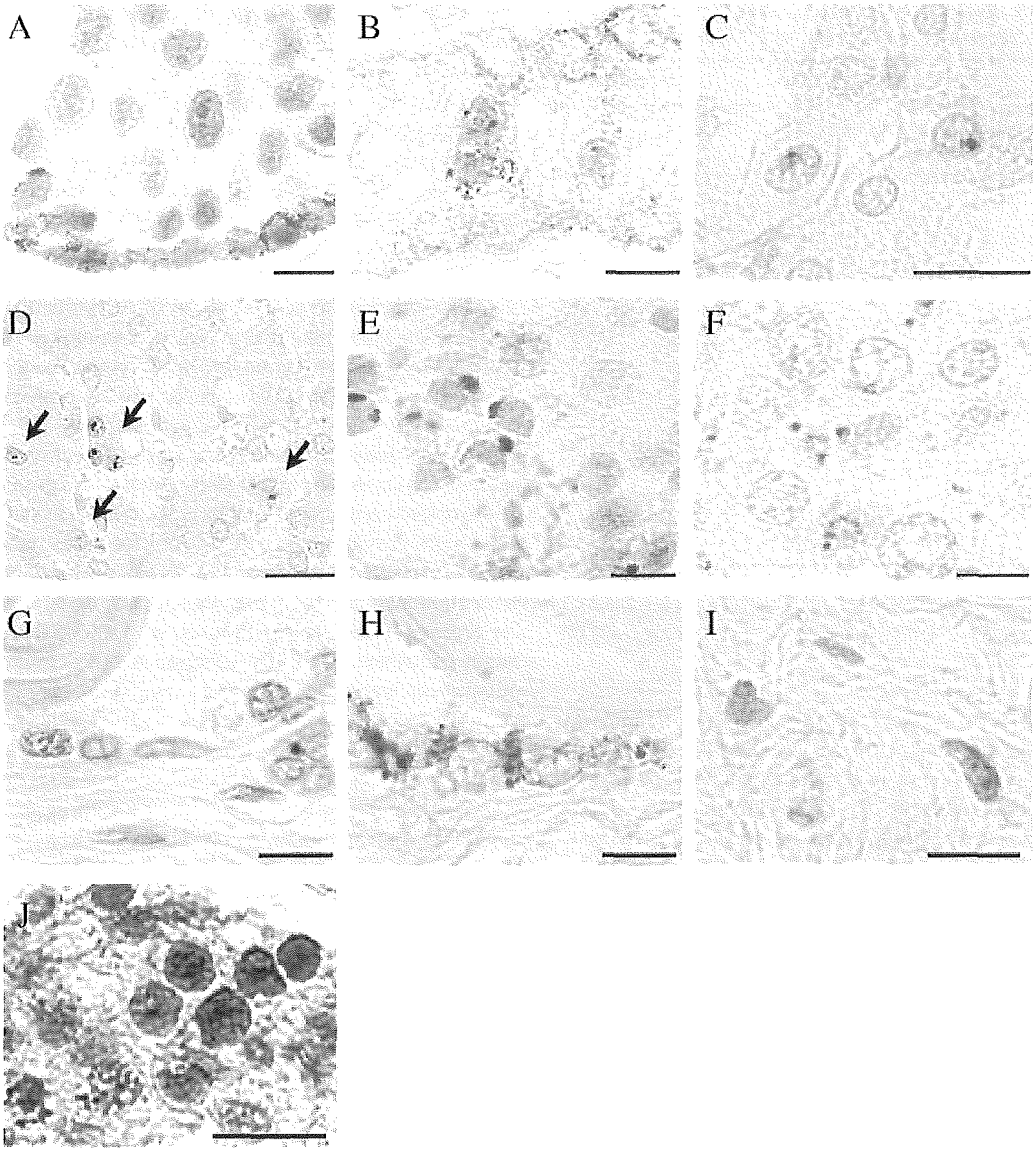

Fig. 5. Immunohistochemical study of the non-neural tissues in SBMA patients using 1C2 antibody. In the non-neural tissues, diffuse nuclear staining and nuclear inclusions are detectable in scrotal skin (**A**), other skin (**B**), proximal tubules of the kidney (**C**), hepatocytes (**D**), Sertoli cells of the testis (**E**), and glandular epithelium (**G**) and fibroblasts of the interstitial connective tissue (**I**) of the prostate gland. Moreover, cytoplasmic inclusions can be detected in hepatocytes (**D**), spermatocytes in the testis (**E**), pancreatic islets of Langerhans (**F**) and glandular epithelium of the prostate gland (**H**). Diffuse nuclear staining is also present using H280 antibody in Sertoli cells of the testis (**J**). Scale bars = 10 μm for **A–C** and **E–I**; and 20 μm for **D** and **J**.

Co-localization of a polyQ-expanded mutant protein with the Golgi apparatus has also been reported for ataxin-2 (Huynh *et al.*, 2003), although the significance of this localization remains unclear. Expression of polyQ-expanded mutant ataxin-2 disrupted the normal morphology of the Golgi complex and increased cell death (Huynh *et al.*, 2003). On the other hand, the lysosomal occurrence of other mutant proteins with an expanded polyQ tract has been reported in DRPLA (Yamada *et al.*, 2002*b*) and Huntington's disease (Sapp *et al.*, 1997). The lysosomal localization of polyQ-expanded mutant proteins suggests a lysosomal autophagic degradation process acting independently of the ubiquitin–proteasome pathway in the polyQ diseases (Sapp *et al.*, 1997). Additionally, the reason why neural tissues develop more nuclear than cytoplasmic accumulation while most involved visceral organs show equal or predominantly cytoplasmic accumulation is unknown. Differences in the predominant degradation pathway dealing with the mutant AR could influence the intracellular site of accumulation and eventual cell toxicity. One important question is whether cytoplasmic mutant AR